Title

Physical positioning markedly enhances brain transduction after intrathecal AAV9 infusion

Journal

Science Advances, 4(11)

ISSN

2375-2548

Authors

Castle, Michael J

Cheng, Yuhsiang

Asokan, Aravind

et al.

Publication Date

2018-11-02

DOI

10.1126/sciadv.aau9859

Peer reviewed

NEUROSCIENCE

Physical positioning markedly enhances brain transduction after intrathecal AAV9 infusion

Michael J. Castle[1]*, Yuhsiang Cheng[1], Aravind Asokan[2,3,4†], Mark H. Tuszynski[1,5]*

Several neurological disorders may benefit from gene therapy. However, even when using the lead vector candidate for intrathecal administration, adeno-associated virus serotype 9 (AAV9), the strength and distribution of gene transfer to the brain are inconsistent. On the basis of preliminary observations that standard intrathecal AAV9 infusions predominantly drive reporter gene expression in brain regions where gravity might cause cerebrospinal fluid to settle, we tested the hypothesis that counteracting vector "settling" through animal positioning would enhance vector delivery to the brain. When rats are either inverted in the Trendelenburg position or continuously rotated after intrathecal AAV9 infusion, we find (i) a significant 15-fold increase in the number of transduced neurons, (ii) a marked increase in gene delivery to cortical regions, and (iii) superior animal-to-animal consistency of gene expression. Entorhinal, prefrontal, frontal, parietal, hippocampal, limbic, and basal forebrain neurons are extensively transduced: 95% of transduced cells are neurons, and greater than 70% are excitatory. These findings provide a novel and simple method for broad gene delivery to the cortex and are of substantial relevance to translational programs for neurological disorders, including Alzheimer's disease and related dementias, stroke, and traumatic brain injury.

INTRODUCTION

Adeno-associated virus (AAV) vectors mediate safe and long-term gene transfer to the brains of rodents, monkeys, and humans (*1*–*3*). AAV-based gene therapies have substantial promise for treatment of neurological disorders such as Alzheimer's disease (AD), Lewy body dementia, frontotemporal dementia, Huntington's disease, stroke, and traumatic brain injury. However, the extensive surface area of the human cortex presents a challenging target for gene delivery. AAV serotype 9 (AAV9) drives widespread central nervous system (CNS) transduction after intrathecal administration to the cerebrospinal fluid (CSF) of nonhuman primates (*4*–*6*). This is a promising technique for gene delivery to the CNS, but stronger gene expression is observed in the spinal cord and dorsal root ganglia (DRGs) than in the brain (*4*, *7*, *8*), and transduction is often variable from subject to subject. After intrathecal infusion of AAV9 or AAVrh.10 in rodents or marmosets, gene expression is observed in the cerebellum, brainstem, olfactory bulb, hippocampus, and entorhinal cortex, but gene transfer to other cortical regions is limited (*9*–*12*). Novel techniques that improve the extent and consistency of intrathecal vector delivery are needed for effective treatment of brain disorders.

Placing adult macaques for 5 or 10 min in the Trendelenburg position, in which the body lies supine on a reclining table with the head approximately 30° below the feet, increases transduction of cervical relative to lumbar spinal cord after intrathecal infusion of AAV9 (*13*). This suggests that gravity affects vector distribution and that positioning the head below the feet may improve delivery to the brain. However, the impact on brain transduction in the macaque was not quantified (*13*), and 10 min in the Trendelenburg position did not increase brain transduction in dogs (*8*). Ten minutes in the Trendelenburg position may thus be insufficient to enhance brain transduction. AAV9 remains detectable in the blood 24 hours after intravenous injection (*14*), indicating that vector binding and uptake occur slowly, and therefore, inversion for longer durations may increase efficacy.

On the basis of these reports, and our initial observation that intrathecal AAV infusion drives gene expression in brain regions where CSF appears to settle under gravity, we hypothesized that 2 hours in the Trendelenburg position after intrathecal AAV9 administration to adult rats would significantly enhance gene delivery to the brain. Because it appears that AAV9 distribution in the CSF is affected by gravity, we also hypothesized that rotating the rat continuously for 2 hours after infusion would prevent the vector from settling under gravity, thereby improving gene transfer to the entire CNS. These simple methods represent a potential means to control and improve gene delivery to the brain after intrathecal AAV9 infusion.

RESULTS

Twenty-one adult rats received a cisterna magna (CM) infusion of 1×10^{12} vector genomes (vg) of AAV9 containing the chicken β-actin (CAG) promoter and enhanced green fluorescent protein (eGFP) transgene, in a total volume of 100 μl. To prevent leakage of vector, 100 μl of CSF was withdrawn from CM before infusion, the infusion site was sealed with fibrin, the vector was infused at a slow rate of 10 μl/min, and the infusion needle remained in place for 10 min after infusion. Seven rats were placed in a typical prone upright position after surgery, with the chin flatly contacting the ground and not tilted to either side ("upright") (Fig. 1A). Seven rats were inverted in a modified Trendelenburg position for 2 hours, with feet 25° above the head and a pillow supporting the head with the scalp parallel to the ground, to prevent gravity from concentrating vector at the rostral apex of the brain ("inverted") (Fig. 1B). Seven rats were secured in a padded enclosure on a disk-style laboratory rotator and were rotated continuously,

[1]Department of Neurosciences, University of California, San Diego, La Jolla, CA 92093, USA. [2]Gene Therapy Center, University of North Carolina at Chapel Hill, Chapel Hill, NC 27599, USA. [3]Department of Genetics, University of North Carolina at Chapel Hill, Chapel Hill, NC 27599, USA. [4]Department of Biochemistry and Biophysics, University of North Carolina at Chapel Hill, Chapel Hill, NC 27599, USA. [5]Veterans Administration Medical Center, San Diego, CA 92161, USA.
*Corresponding author. Email: mcastle@ucsd.edu (M.J.C.); mtuszynski@ucsd.edu (M.H.T.)
†Present address: Department of Surgery, Department of Molecular Genetics and Microbiology, Duke University School of Medicine, 203 Research Drive, MSRB1, Durham, NC 27710, USA.

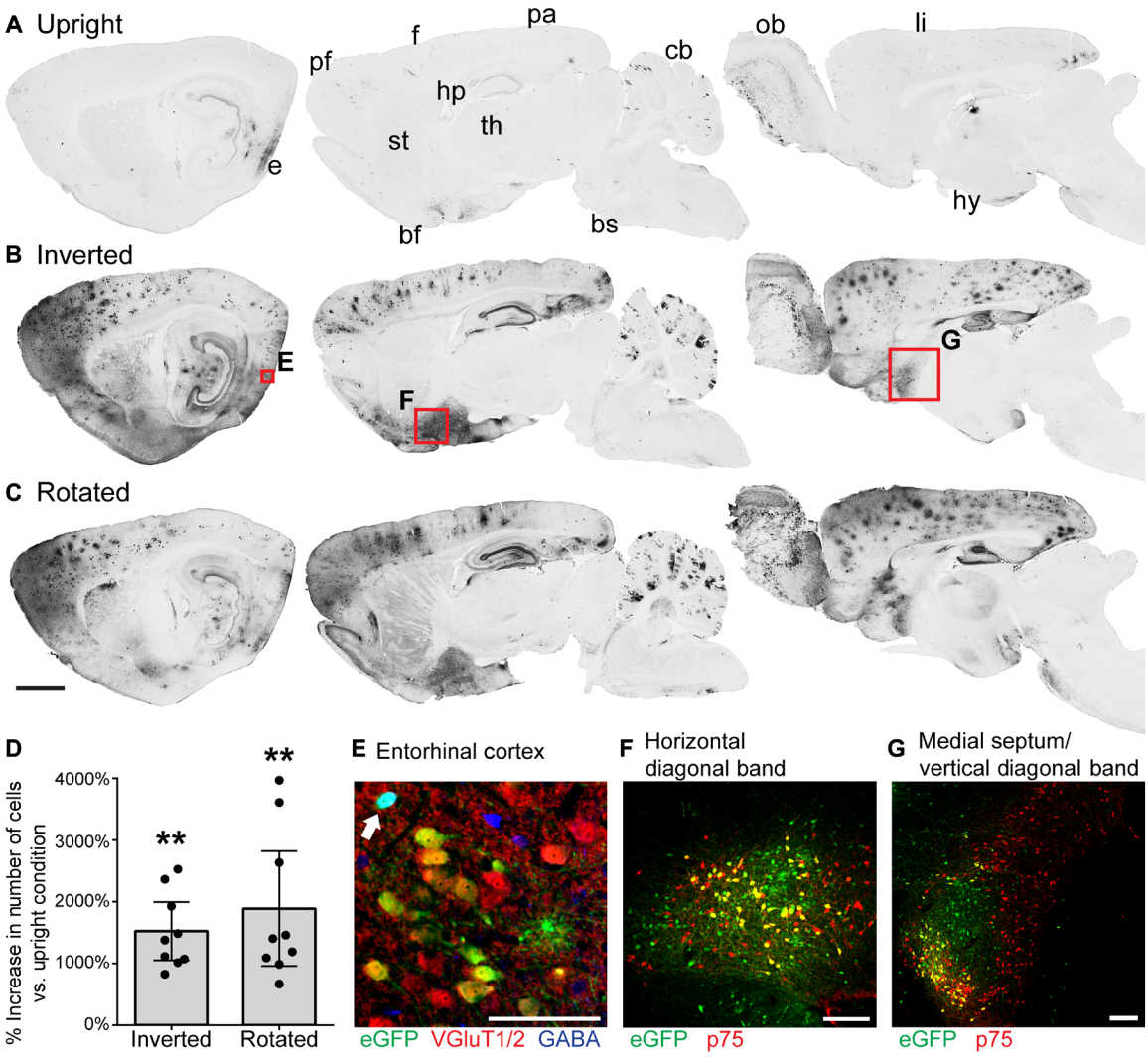

Fig. 1. Inversion and rotation greatly enhance gene transfer to the brain after intrathecal AAV9 infusion. (**A** to **C**) GFP labeling in 40-μm-thick sagittal brain sections in rats that received intrathecal AAV9-CAG-eGFP, and (A) remained upright for 2 hours, (B) were inverted for 2 hours or (C) were rotated for 2 hours after surgery. From left to right, sections are 0.5, 2.5, and 4.5 mm lateral from bregma. Both inversion and rotation substantially increased gene transfer to entorhinal (e), prefrontal (pf), frontal (f), parietal (pa), and limbic (li) cortices, as well as hippocampus (hp), basal forebrain (bf), cerebellum (cb), and olfactory bulb (ob). There was minimal gene transfer to striatum (st), thalamus (th), hypothalamus (hy), and brainstem (bs). Scale bar, 2 mm. (**D**) The average increase in the number of GFP-positive cells per section in inverted or rotated animals relative to upright animals is shown for nine brain regions: prefrontal, frontal, parietal, entorhinal, and limbic cortices, as well as hippocampus, subiculum, horizontal diagonal band, and medial septum/vertical diagonal band. Inversion and rotation increased the number of GFP-positive cells by an average of 1520 and 1890%, respectively, relative to upright animals. This increase was highly significant as determined by Friedman test ($P = 0.0003$) and Tukey's post tests. Error bars represent the 95% confidence interval. $^{**}P \leq 0.01$. (**E**) Following inversion for 2 hours, 73.0% of transduced neurons in the entorhinal cortex are excitatory glutamatergic neurons, and 27.0% are inhibitory GABAergic neurons (arrow). The image is a single optical section acquired with structured illumination. (**F**) In the cholinergic basal forebrain, inversion for 2 hours induces GFP expression in 22.5% of cholinergic neurons in the horizontal diagonal band and (**G**) 13.9% of cholinergic neurons in the medial septum/vertical diagonal band (MS/VDB), based on colocalization with p75. Scale bars, 100 μm (E to G).

alternating between upright and inverted positions, for 2 hours at a rate of 20 rpm ("rotated") (Fig. 1C). After 2 hours, all rats were returned to housing in an upright position. Rats were euthanized 4 weeks after surgery, and gene transfer to the brain was examined using immunolabeling for GFP (Fig. 1).

Inversion and rotation both markedly enhanced gene transfer to the brain after intrathecal AAV9 infusion (Fig. 1, A to C). Notably, after inversion or rotation, gene transfer was strongly biased for the cerebral cortex and basal forebrain, the brain regions that are primarily affected in dementias, stroke, and traumatic brain injury. Relative to upright animals, the mean number of GFP-positive cells increased by an average of 1520% after inversion and 1890% after rotation in nine regions of cortex and basal forebrain (Fig. 1D). These increases were highly significant (Fig. 1D). The olfactory bulb and cerebellum were also strongly transduced (Fig. 1, A to C). Minimal gene expression was observed throughout the rest of the brain.

Transduction of cholinergic basal forebrain was extensive: Among the three inverted rats with gene expression closest to the mean, 22.5% (SD = 14.0%) of cholinergic neurons in the horizontal limb of the diagonal band were GFP positive, as well as 13.9% (SD = 7.93%)

in the medial septum/vertical limb of the diagonal band (MS/VDB; Fig. 1, F and G). In contrast, transduction of dopaminergic and serotonergic brain regions was minimal: 0.72% (SD = 0.89%) of dopaminergic neurons in substantia nigra (SN) were GFP positive, 0.49% (SD = 0.22%) in the ventral tegmental area (VTA), and 0.58% (SD = 0.82%) in hypothalamus. No serotonergic neurons in the raphe nuclei were GFP positive.

Within cortex, 73.0% of GFP-positive neurons were excitatory and 27.0% were inhibitory (SD = 12.0%; Fig. 1E), as determined by colocalization with the excitatory marker vesicular glutamate transporter 1/2 (VGluT1/2) and the inhibitory marker γ-aminobutyric acid (GABA). A minority of GFP-positive neurons did not colocalize with either VGluT1/2 or GABA (19.1%; SD = 8.15%). Although some uncolocalized GFP-positive neurons were likely GABAergic, as GABA antibodies do not stain every GABAergic neuron (*15*), others had pyramidal morphology, indicating an excitatory transmitter phenotype. Uncolocalized neurons were therefore not included in the final counts. These results closely match the population of 70 to 85% excitatory pyramidal neurons and 15 to 30% inhibitory interneurons in the rat cortex (*16*), suggesting that AAV9 was not biased for transduction of either cortical neuron subtype.

Gene expression was quite variable among rats that were placed in an upright position after intrathecal AAV9 infusion. Inversion and rotation both greatly improved the animal-to-animal consistency of neuronal gene transfer (Fig. 2). The strongest gene expression was observed in the entorhinal cortex but was highly variable among

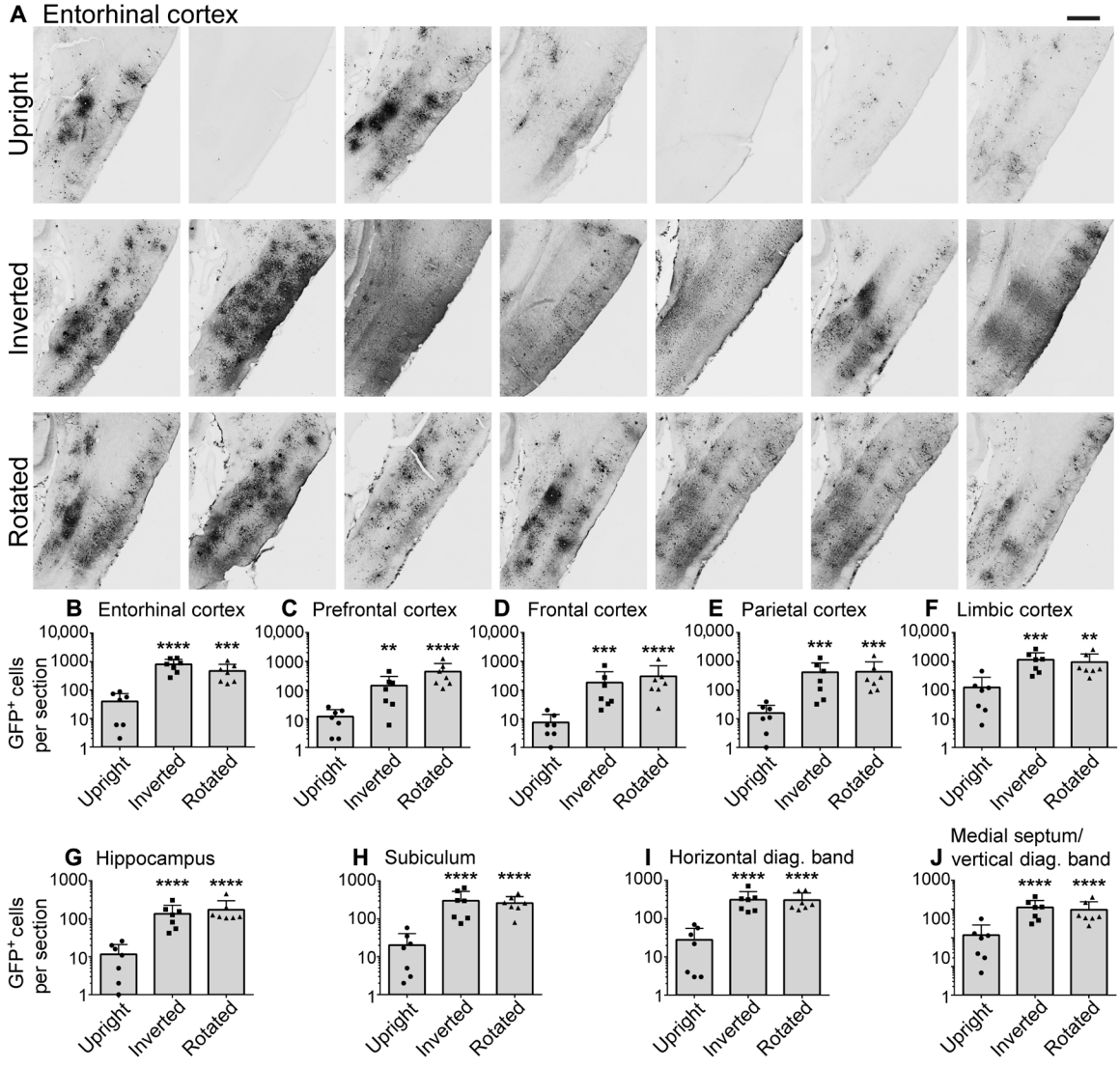

Fig. 2. Inversion and rotation improve the extent and consistency of gene transfer to cerebral cortex and basal forebrain after intrathecal AAV9 infusion. (**A**) GFP labeling in medial entorhinal cortex of every animal in the study after intrathecal infusion. GFP expression among rats that remained upright after intrathecal AAV9 infusion was highly variable and minimal in some animals. Gene expression in rats that were inverted or rotated for 2 hours after surgery was both more extensive and more consistent, with robust entorhinal transduction in all 14 animals. Rostral is left in all images. Scale bar, 500 μm. (**B** to **I**) Inversion and rotation significantly and substantially enhanced gene transfer to all regions of cortex and basal forebrain. $n = 7$ rats per cohort. $^{****}P \leq 0.0001$, $^{***}P \leq 0.001$, $^{**}P \leq 0.01$: significance of comparison to upright group by one-way analysis of variance (ANOVA) and Tukey's post test. No significant differences were detected between inverted and rotated rats. Error bars represent SD. *Y* axes are plotted on a logarithmic scale.

individual subjects in the upright group (Fig. 2A). In contrast, gene transfer to entorhinal cortex was consistently strong across all 14 rats that were inverted or rotated after intrathecal AAV9 infusion (Fig. 2A). Inversion and rotation increased the average number of GFP-positive cells in entorhinal cortex more than 10-fold relative to animals that recovered in an upright position (Fig. 2B).

Moreover, inversion and rotation markedly improved transduction of all other examined brain regions (Fig. 2, C to J). In addition to entorhinal cortex, inversion and rotation also greatly increased the number of GFP-positive cells in prefrontal, frontal, parietal, and limbic cortices, as well as hippocampus, subiculum, horizontal limb of the diagonal band, and MS/VDB (Fig. 2, C to J). This increase was highly significant in every brain region, and no significant differences between inverted and rotated rats were detected.

Most GFP-positive cells in the brain were neurons, and transduction of glia was minimal (Fig. 3): 95.5% (SD = 2.34%) of GFP-positive cells were neurons (Fig. 3A), while only 0.779% (SD = 1.09%) of GFP-positive cells were astrocytes and 4.39% (SD = 4.37%) were oligodendrocytes (Fig. 3, B and C). No microglia were transduced (Fig. 3D). Neurons, astrocytes, and oligodendrocytes therefore account for all transduced cells in the brain, with greater than 95% of GFP-positive cells being neurons.

Microglia and astrocytes exhibited normal resting morphology in treated animals, and no infiltration of transduced brain regions by reactive microglia or astrocytes was observed, preliminarily suggesting that intrathecal AAV9 infusion is well tolerated (fig. S1). Daily animal monitoring also did not detect clinically evident toxicity over the experimental time period of 4 weeks.

Fewer cells were transduced in spinal cord than in brain (fig. S2A): 11.2 (SD = 12.8) cells per section among all spinal levels in upright animals, 31.4 (SD = 22.3), in inverted animals, and 35.8 (SD = 22.4) in rotated animals. Significantly more cervical spinal cord cells were transduced after inversion ($P < 0.001$) or rotation ($P < 0.01$) than after upright recovery: 56.8 (SD = 22.4) cells per cervical section in inverted animals, 52.5 (SD = 27.6) in rotated animals, and 18.4 (SD = 15.3) in upright animals.

Inversion and rotation enhanced cervical gene transfer in distinct ways: Inversion strongly biased gene transfer for cervical spinal cord, while rotation distributed gene transfer evenly among spinal levels. Inverted animals had 56.8 (SD = 22.4) GFP-positive cells per section in cervical spinal cord, significantly more than thoracic (27.0 cells per section, SD = 14.3, $P < 0.05$), lumbar (17.2 cells per section, SD = 10.7, $P < 0.001$), or sacral spinal cord (24.6 cells per section, SD = 18.8, $P < 0.01$). In contrast, rotated animals had 52.5 (SD = 27.6) GFP-positive cells per section in cervical spinal cord, which was not significantly different than thoracic (33.3 cells per section, SD = 19.1), lumbar (28.6 cells per section, SD = 21.1), or sacral spinal cord (28.9 cells per section, SD = 15.5). The increased homogeneity of gene transfer throughout the spinal cord following rotation could be beneficial for gene therapies directed at the entire nervous system.

Gene expression in the spinal cord was largely restricted to dorsal horn layers I and II and dorsal white matter. A majority of GFP-positive cells were located in dorsal spinal cord among all conditions (82.5%). Neurons in the superficial layers of the dorsal horn were preferentially transduced (fig. S2B), which may be due to the proximity of these neurons to the surface of the spinal cord and greater accessibility to vector in the CSF. Transduction of cells in the ventral horn, including α motor neurons, was limited in number (fig. S2, C and D). There was an average of 0.74 (SD = 1.05) GFP-positive ventral neurons per section among all groups and spinal levels, and only 5.7% of GFP-positive neurons were located in ventral spinal cord. Furthermore, only 36.9% of GFP-positive ventral neurons colocalized with choline acetyltransferase (ChAT), and only an average of 0.25 (SD = 0.32) ventral neurons per section expressed both GFP and ChAT (fig. S2D). Transduction of ChAT-positive α motor neurons and commissural interneurons was therefore rare.

Inversion ($P \leq 0.05$) and rotation ($P \leq 0.01$) significantly increased vector distribution to cervical DRGs compared to upright animals (Fig. 4). Only 4.22% (SD = 6.08%) of cervical DRG neurons and 11.4% (SD = 12.0%) of lumbar DRG neurons were GFP positive after upright recovery. In contrast, 24.8% (SD = 13.6%) of cervical DRG neurons and 30.6% (SD = 26.9%) of lumbar DRG neurons were GFP positive

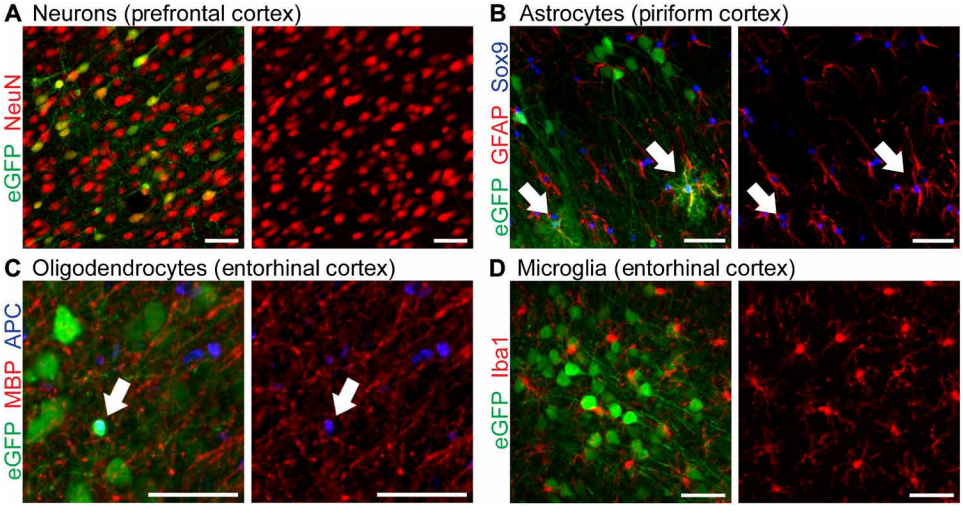

Fig. 3. AAV9-mediated gene transfer in the brain is predominately targeted to neurons. (**A** to **D**) Intrathecal AAV9 infusion and inversion for 2 hours: (A) 95.5% of GFP-labeled cells are neurons, by colocalization with neuronal nuclei (NeuN); (B) 0.779% of GFP-labeled cells are astrocytes, by colocalization with glial fibrillary acidic protein (GFAP) and sex-determining region Y-box9 (Sox9); and (C) 4.39% of GFP-labeled cells are oligodendrocytes, by colocalization with adenomatous polyposis coli (APC). (D) No microglia were transduced by colocalization with ionized calcium-binding adapter molecule 1 (Iba1). Scale bars, 50 μm.

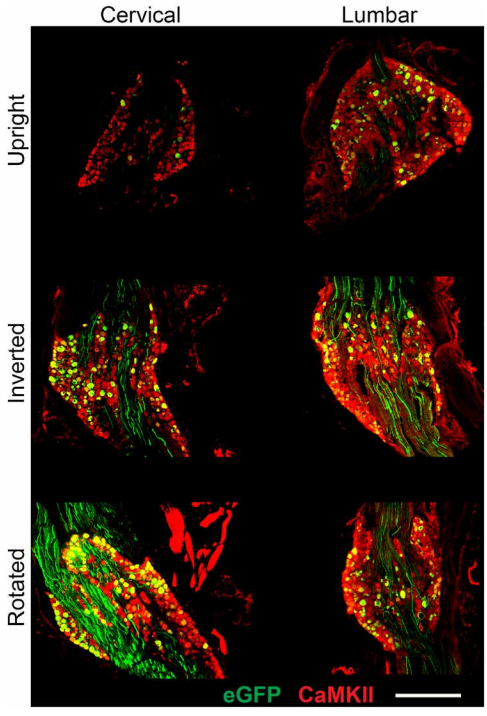

Fig. 4. Inversion and rotation enhance gene transfer to cervical DRG. In rats that were either inverted or rotated after intrathecal AAV9 infusion, significantly more cervical DRG cells were transduced than in rats that remained upright. Nearly all transduced cells were neurons by colocalization with CaMKII (99.5%), including both small- and large-diameter DRG neurons. Scale bar, 500 μm.

after inversion, and 29.7% (SD = 16.4%) of cervical DRG neurons and 28.9% (SD = 31.5%) of lumbar DRG neurons were GFP positive after rotation. Nearly all GFP-positive DRG cells were neurons (99.5%), as determined by colocalization with Ca^{2+}/calmodulin-dependent protein kinase II (CaMKII), which labels all DRG neurons (Fig. 4) (*17*). Efficient gene delivery to DRG neurons can be important in the development of clinical gene therapies for chronic pain (*18*, *19*).

DISCUSSION

Intrathecal AAV9 infusion followed by 2 hours in the inverted Trendelenburg position represents a simple, minimally invasive, and highly effective method for increasing the extent and consistency of gene delivery to the brain. The number of transduced cells increased more than 15-fold in most regions of the cortex and basal forebrain. More than 95% of transduced cells are neurons, and more than 70% of transduced neurons are excitatory. While standard intrathecal or systemic delivery of AAV9 also transduces the brain, these approaches vary from subject to subject and lack the specificity and robustness of expression identified in this study.

Gene expression in the upright cohort was highly variable. This is consistent with previous reports of intrathecal AAV9 infusion, which relied on qualitative description and polymerase chain reaction–based measurement of vector genomes in limited numbers of animals, and did not directly quantify the number of transduced cells in the brain (*4*–*13*). To our knowledge, our data represent the first quantitative analysis of the number of transduced brain cells after intrathecal AAV9 infusion in large cohorts, as well as the first demonstration of a simple positioning method through which the strength and consistency of gene transfer to the brain can be enhanced. Although 10 min of Trendelenburg positioning was previously reported to increase transduction of cervical spinal cord after intrathecal AAV9 infusion in macaques (*13*), this short duration did not increase transduction of the brain (*8*). We have shown not only that a longer duration of 2 hours in the Trendelenburg position enhances gene transfer to the brain in addition to cervical spinal cord but also that the number of transduced brain cells is significantly increased by more than 15-fold. This has broad importance for ongoing and future clinical trials using intrathecal AAV9 infusion, which may consider extended-duration Trendelenburg positioning to improve gene delivery to the brain.

These findings have particular importance for the treatment of AD and related dementias, as our technique targets the cerebral cortex and basal forebrain with remarkable specificity. Gene expression among all groups was strongest in the entorhinal cortex, which is among the earliest affected brain regions in AD. Gene expression may have been strongest in entorhinal cortex because this cortical region is adjacent to the site of CSF absorption from the subarachnoid space into the venous system. CSF is normally formed in the lateral, third, and fourth ventricles, flows caudally, and then continues upward over the cerebral convexities for absorption into the superior sagittal sinus (*20*). Vector could accumulate near the entorhinal cortex because this region represents a "dead end" for CSF flow before absorption into the venous system and because vector particles settle under gravity toward the most inferior aspect of the middle cranial fossa where the entorhinal cortex is located.

Gene expression was consistently strong in the cholinergic basal forebrain, which is also among the earliest affected brain regions in AD. In this study, 14.3% of transduced neurons in the diagonal band of Broca were cholinergic; previous studies demonstrated that 14.5% of all neurons in the rat diagonal band are cholinergic (*21*). This suggests that there is not a specific bias for transduction of cholinergic neurons, and thus, preferential transduction of basal forebrain is not due to a greater affinity of AAV9 for cholinergic neurons or to a greater activity of the CAG promoter in cholinergic neurons. It is possible that the extensive arterial vascularization of the anterior perforated substance in basal forebrain affords greater accessibility to AAV9 (*22*), which is hypothesized to enter the brain parenchyma by CSF flow through the Virchow-Robin spaces surrounding the penetrating arteries of the brain (*9*, *10*, *12*, *23*). We observed perivascular clusters of transduced cells in some cortical regions, as previously described (*5*, *12*). Clustering of transduced cells is not due to vector tropism: Gene expression is distributed evenly when this vector is injected directly into the adult rat cortex (fig. S3).

Intravenous AAV infusion may also transduce the brain and is a potential alternative to intrathecal AAV9 infusion. However, systemic AAV9 infusion results in extensive gene transfer to non-neural tissues, is sensitive to preexisting anti-AAV9 antibodies, transduces more astrocytes than neurons in adults, and requires high AAV9 doses to efficiently transduce the CNS, ranging as high as 1.0×10^{14} vg/kg in rodents and 2.0×10^{14} vg/kg in humans (*14*, *24*, *25*). While broad glial, neuronal, and systemic transduction could be useful for gene replacement in metabolic disorders, broad non-neuronal gene expression may be undesirable for therapeutic delivery of nervous system growth factors or neurotransmitter-synthesizing enzymes (*26*–*29*). AAV-PhP.B and AAV-PhP.eB, two vectors produced by cre-dependent directed evolution, have less systemic

tropism and transduce adult mouse neurons more broadly than AAV9 at reduced intravenous doses of ~4×10^{12} vg/kg (*30*, *31*). However, AAV-PhP.B is not more effective than AAV9 in macaques, and it remains to be determined whether these PhP vectors will be clinically practical (*32*, *33*).

Intrathecal AAV9 infusion with 2 hours of inversion broadly transduces the cortex at a dose of ~6×10^{12} vg/kg, less than the maximum dose of ~1×10^{13} vg/kg used in two ongoing phase 1 trials of intrathecal AAV9 infusion (*34*, *35*). This technique is therefore readily scalable for clinical use. Preclinical and clinical studies suggest that this dose range is safe, and we did not detect toxicity in the rat brain by immunolabeling of microglia and astrocytes. Intravenous coadministration of mannitol, which may enhance interstitial diffusion of AAV after intrathecal delivery, could further increase transduction (*10*, *36*). In humans, transduction may also be increased if the patient sleeps in an inverted position after recovery from anesthesia because sleep increases cortical CSF influx (*37*).

There are several promising gene therapies for AD, including the neuroprotective growth factor brain-derived neurotrophic factor and the amyloid-targeted proteolytic enzymes neprilysin-s and apolipoprotein E2 (*27*, *38*–*40*). These therapeutic proteins are secreted from transduced brain cells, further broadening the range of delivery. Combined with the widespread gene transfer that we report after intrathecal AAV9 infusion, a secreted protein could treat the cerebral cortex and basal forebrain extensively. This simple and novel intrathecal delivery technique thus represents a potentially important advance in gene delivery for cortical disorders, including AD, stroke, and traumatic brain injury.

MATERIALS AND METHODS

Study design

We hypothesized that the number of transduced cells in the brain, cervical spinal cord, and cervical DRG would be greater in rats that were inverted or rotated for 2 hours following intrathecal AAV9 infusion than in rats that recovered in an upright position. This hypothesis was tested in 25 adult female Fischer F344 rats (Harlan Laboratories). Four animals with failed surgeries were excluded and euthanized at the time of surgery; no other animals were excluded from this study. The remaining 21 rats were assigned proportionally to one of the following cohorts: upright, rotated, and inverted. All rats were assigned to their cohort before surgery, and the order was mixed sequentially among cohorts. Rats were sacrificed 4 weeks after treatment. The number of transduced cells in the brain, spinal cord, and DRG was quantified by histology. Brains and spinal cords from all 21 animals were quantified equally, with no exclusions. Cervical DRGs from 20 animals and lumbar DRGs from 13 animals were quantified: Animals were excluded if sections containing at least 150 neurons from three different DRGs were not obtained. For all analyses, the number of quantified images was determined in advance and was not altered. All quantified data were included, and no outliers were excluded. Investigators were fully blinded to the identity of all images during quantification.

Study approval

Animal experiments conformed to the National Institutes of Health Guide for the Care and Use of Laboratory Animals and were performed under protocols approved by the Institutional Animal Care and Use Committee of the Veteran's Administration San Diego Healthcare System.

Surgical procedures

Rats were 9 to 12 weeks old at the time of surgery. Rats were anesthetized by intraperitoneal injection of KXA [ketamine (50 mg/kg), xylazine (2.6 mg/kg), and acepromazine (0.5 mg/kg)], followed by booster injections as needed. Heat support was provided until animals recovered from anesthesia. Fur was shaved from the occipital crest to the base of the neck, and animals were mounted in a stereotactic frame (Kopf Instruments), with the head at a 45° angle to provide a straight needle path into CM. Using a #15 scalpel, an incision was made along the midline from the occipital crest to the C1 vertebra. The incision was held open with a surgical retractor, exposing the dura overlying CM. Remaining muscle was removed from the dura using a freer elevator.

A 1-ml plastic syringe with a sterile, single-use 30-g beveled needle was mounted on a syringe pump (Chemyx #10050) attached to the stereotactic frame. The needle was inserted through the dura at midline proximal to the C1 vertebra and then lowered 0.5 mm into CM. Using the syringe pump, 100 µl of CSF was withdrawn at a rate of 20 µl/min. The needle was then withdrawn from the animal, and the plastic syringe was removed from the syringe pump. One hundred microliters of AAV9-CAG-eGFP (1×10^{13} vg/ml) was drawn into a 100-µl glass syringe with a 30-g blunt needle (Hamilton #7656-01 and #7762-03), and the syringe was mounted on the pump. The blunt needle was then gently inserted through the hole in the dura previously made by the beveled needle, using fine forceps to guide the needle and ensure a tight seal, and lowered 0.6 mm into CM. The dura was dried with a cotton-tipped applicator, and 20 µl of rat thrombin (100 IU/ml; MilliporeSigma #T5772) was mixed in a micropipette with 20 µl of rat fibrinogen (50 mg/ml; MilliporeSigma #F6755) to form fibrin and then immediately applied to the incision above the needle hole. Thrombin and fibrinogen were resuspended in sterile saline before surgery and stored at −80°C. After the fibrin had set for a least 5 min and was observed to be gelatinous, 100 µl of AAV9 was infused at a rate of 10 µl/min. The needle was withdrawn after a 10-min delay to allow pressure to dissipate, minimizing backflow during withdrawal. The muscle was sutured, and the skin was closed with wound clips.

The infusion was monitored continuously to ensure that leakage did not occur. In two rats, the dura did not seal tightly around the infusion needle, and leakage was observed. In two additional rats, the dura was torn during surgery, and infusion was not attempted. These four rats were excluded from the study and euthanized. After surgery, rats in the upright cohort were placed on their stomach in a prone position and were monitored for at least 2 hours to ensure that upright posture was maintained and that the head did not tilt to either side. Rats in the inverted cohort were placed on their back on a soft platform with feet 25° above the head for 2 hours. The head was supported parallel to the floor by cotton padding. The platform was housed in an incubator for heat support. Rats in the rotation cohort were placed in a padded enclosure on a disk-style laboratory rotator (Glas-Col #099ARD4512) and were held securely in place by a removable cotton pillow. Reusable hand warmers were added to the enclosure to provide heat support. Rats were rotated at 20 rpm for 2 hours, alternating between upright and inverted positions. All animals were continuously monitored to ensure adequate anesthesia and warmth throughout the above procedures.

AAV vectors

Recombinant AAV9 vectors were generated as described (*23*).

Tissue dissection and processing

Four weeks after surgery, all rats received a terminal dose of KXA anesthesia and were transcardially perfused with 300 ml of ice-cold 0.1 M phosphate-buffered saline (pH 7.4). Brains were severed from the spinal cord at the level of the C1 vertebra, removed completely from the skull, drop-fixed for 48 hours in 4% paraformaldehyde (PFA) in 0.1 M phosphate buffer at 4°C, and cryoprotected for at least 72 hours in 30% sucrose at 4°C. Vertebral columns were dissected, drop-fixed for 48 hours in 4% PFA at 4°C, and cryoprotected for at least 72 hours in 30% sucrose at 4°C. Half-inch segments of cervical, mid-thoracic, and lumbar/sacral spinal cord, as well as cervical and lumbar DRGs, were dissected from the vertebral columns and stored in 30% sucrose. Brains were sectioned sagittally, and spinal cords were sectioned transversely on a sliding microtome set to a thickness of 40 μm. Free-floating sections were serially collected. Each brain series comprised every 12th section from one hemisphere, and each spinal cord series comprised every 24th section from one segment. Three DRGs from each spinal level were blocked in optimal cutting temperature compound, sectioned on a cryostat set to a thickness of 20 μm, and mounted on gelatin-coated slides. Slides comprised every sixth section from cervical DRGs and every fourth section from lumbar DRGs.

Immunohistochemistry

For light-level immunohistochemistry, free-floating brain sections were washed in tris-buffered saline (TBS), incubated in 50% methanol in TBS for 5 min, incubated in 100% methanol for 30 min, incubated in 50% methanol in TBS for 5 min, washed in TBS, blocked in 5% donkey serum and 0.25% Triton X-100 in TBS for 1 hour, and incubated in rabbit polyclonal anti-GFP primary antibody (1:10,000; Invitrogen Thermo Fisher Scientific #A11122) diluted in blocking solution overnight at 4°C. The next day, sections were washed in TBS, incubated in donkey anti-rabbit biotinylated secondary antibody (1:200; Jackson ImmunoResearch #711-065-152) in blocking solution for 2 hours at room temperature, washed in TBS, incubated in VECTASTAIN ABC peroxidase (Vector Laboratories #PK-6100) for 1 hour at room temperature, and washed in TBS. Sections were then developed for 7 min in TBS containing 3,3-diamino-benzidine-HCl (0.25 mg/ml; MilliporeSigma #5637), 0.04% $NiCl_2$, and 0.015% H_2O_2, washed in TBS, dehydrated, and coverslipped in DPX mounting medium (MilliporeSigma #06522).

For fluorescent immunohistochemistry, free-floating brain or spinal cord sections were washed in TBS, blocked in 5% donkey serum and 0.25% Triton X-100 in TBS for 1 hour, and incubated in primary antibody diluted in blocking solution overnight at 4°C. The next day, sections were washed in TBS, incubated in donkey Alexa Fluor 488–, Alexa Fluor 555–, or Alexa Fluor 647–conjugated secondary antibodies (1:500; Invitrogen Thermo Fisher Scientific and Jackson ImmunoResearch), incubated for 10 min in 4′,6-diamidino-2-phenylindole (DAPI; 0.5 μg/ml; Invitrogen Thermo Fisher Scientific #D1306) in TBS, washed in TBS, and coverslipped in Mowiol mounting medium prepared as described (*41*). The following antibodies were used for fluorescent staining of brain: chicken polyclonal anti-GFP (1:1000; Aves Labs #GFP-1020), rabbit polyclonal anti-GFP (1:1000; Invitrogen Thermo Fisher Scientific #A6455), goat polyclonal anti-Sox9 (1:500; R&D Systems #AF3075), chicken polyclonal anti-GFAP (1:2000; EnCor Biotechnology #CPCA-GFAP), mouse monoclonal anti-APC (1:400; MilliporeSigma #OP80), mouse monoclonal anti–myelin basic protein (MBP; 1:1000; EnCor Biotechnology #MCA-7G7), rabbit polyclonal anti-Iba1 (1:800; Wako #019-19741), rabbit polyclonal anti-NeuN (1:500; Biosensis #R3770), guinea pig polyclonal anti-VGluT1 (1:1000; MilliporeSigma #AB5905), guinea pig polyclonal anti-VGluT2 (1:1000; MilliporeSigma #AB2251), rabbit polyclonal anti-GABA (1:500; MilliporeSigma #A2052), mouse monoclonal anti–rat endothelial cell antigen-1 (RECA-1) (1:100; Abcam #ab9774), mouse monoclonal anti–tyrosine hydroxylase (TH) (1:1000; MilliporeSigma #MAB318), rabbit polyclonal anti-serotonin [5-hydroxytryptamine (5-HT)] (1:500; ImmunoStar #20080), and mouse monoclonal anti-p75 (1:1000; MilliporeSigma #MAB365). The following antibodies were used for fluorescent staining of spinal cord: chicken polyclonal anti-GFP (1:1000; Aves Labs #GFP-1020), goat polyclonal anti-ChAT (1:500; Genetex #GTX82725), and mouse monoclonal anti-NeuN (1:500; MilliporeSigma #MAB377).

An identical protocol was used to perform fluorescent immunohistochemistry on DRGs. Washes and solutions were applied to DRG slides using a Sequenza immunostaining system (Electron Microscopy Sciences #71407-01). The following antibodies were used for fluorescent staining of DRG: chicken polyclonal anti-GFP (1:1000; Aves Labs #GFP-1020) and rabbit monoclonal anti-CaMK2 (1:500; Genetex #GTX61641).

Microscopy

All microscopy was performed using a Keyence BZ-X710 all-in-one fluorescence microscope. Images of brain sections stained with light-level immunohistochemistry were acquired using a 10× Plan-Apo objective and bright-field microscopy. Images of DRG sections were acquired using a 20× Plan-Apo objective and fluorescent microscopy. *Z*-stacks of brain sections fluorescently stained against TH, p75, or 5-HT were acquired using a 10× Plan-Apo objective and a slice interval of 1.5 μm. *Z*-stacks of all spinal cord sections, and of brain sections fluorescently stained against GFAP, Sox9, APC, MBP, Iba1, NeuN, GABA, VGluT1/2, or RECA-1, were acquired using a 20× Plan-Apo objective, a slice interval of 0.4 μm, and structured illumination (one-dimensional slit; width, 10). Maximum intensity projections were used for display and analysis of all *z*-stacks, except for brains stained against GABA and VGluT1/2, for which single optical sections were used. Keyence BZ-X Analyzer software was used to generate maximum intensity projections and perform automated stitching.

Quantification

Investigators were fully blinded to the identity of all quantified images. Quantification was performed by M.J.C. and Y.C.: Experiments quantified by M.J.C. were blinded by Y.C., and experiments quantified by Y.C. were blinded by M.J.C. ImageJ with Cell Counter plugin was used for all quantification.

Brain transduction after intrathecal infusion of AAV9 was quantified in 40-μm sagittal brain sections stained against GFP (Figs. 1D and 2, B to J). Brain regions were identified using a rat brain atlas (*42*), and an equivalent sagittal brain section from each animal was used for quantification. Entorhinal cortex was quantified using sections 5 mm lateral from bregma; hippocampus and parietal cortex were quantified using sections 4 mm lateral from bregma; frontal cortex, prefrontal cortex, HDB, and subiculum and subiculum were quantified using sections 2.5 mm lateral from bregma; and limbic cortex and MS/VDB were quantified using sections 0.5 mm lateral from bregma. The total number of GFP-positive cells in one 40-μm section of each brain region was counted for each rat ($n = 7$ rats per cohort) (Fig. 2, B to J). The mean number of GFP-positive cells in each brain region was determined for each cohort, and the percent increase in the mean relative to the upright cohort was

calculated for the inverted and rotated cohorts in each brain region (n = 9 brain regions; Fig. 1D).

Spinal cord transduction was quantified in 40-μm transverse sections stained against GFP, NeuN, ChAT, and DAPI (Fig. 4A). Cervical, thoracic, lumbar, and sacral spinal cord were analyzed. The number of GFP-positive cells in dorsal spinal cord was counted in three randomly selected sections from each spinal level. The number of GFP-positive cells in ventral spinal cord was counted in all sections from a 1-in-24 series of tissue sections at each spinal level. Animals frequently exhibited less than one GFP-positive ventral neuron per three sections, and thus, the entire series was quantified to obtain an accurate count. Neurons were identified by colocalization with NeuN; motor neurons and motor interneurons were identified by colocalization with both NeuN and ChAT; and glia were identified by colocalization with DAPI but not with NeuN. From these counts, the number of GFP-positive cells, neurons, and motor neurons in dorsal or in ventral spinal cord per 40-μm transverse section was calculated at each spinal level for each rat (n = 7 rats per cohort).

DRG transduction was quantified in 20-μm sections stained against GFP, CaMK2, and DAPI (Fig. 4B). For each animal, sections from three different cervical DRGs and three different lumbar DRGs were quantified. The most central section from each DRG, defined as the section with the most CaMK2-positive neurons, was used for analysis. In each section, the number of CaMK2-positive neurons, the number of GFP-positive/CaMK2-positive transduced neurons, and the number of GFP-positive/CaMK2-negative/DAPI-positive transduced glia were counted. From these counts, the average number of total neurons, transduced neurons, and transduced glia per 20-μm section was quantified for each rat (n = 7 rats per cohort), and the average percentage of neurons transduced was calculated. Rats were excluded from analysis if sections containing at least 150 neurons from three different DRGs were not obtained. Cervical DRGs from n = 6 and lumbar DRGs from n = 4 upright rats, cervical DRGs from n = 7 and lumbar DRGs from n = 5 inverted rats, and cervical DRGs from n = 7 and lumbar DRGs from n = 5 rotated rats were quantified.

Relative transduction of neurons, astrocytes, oligodendrocytes, and microglia in the brain was quantified in 40-μm sagittal brain sections stained against GFP and DAPI, as well as NeuN for neurons, Sox9 and GFAP for astrocytes, APC and MBP for oligodendrocytes, and Iba1 for microglia (Fig. 3). Astrocyte and microglia images were quantified by M.J.C., and oligodendrocyte and neuron images were quantified by Y.C., with each blinded to the other's results. The three rats in the inverted cohort with total GFP expression closest to the mean, as quantified above, were used for analysis. For each cell type, six different brain regions were quantified from each animal (18 images in total). Neurons, oligodendrocytes, and microglia were quantified in entorhinal cortex, frontal cortex, temporal cortex, hippocampus, subiculum, and HDB. Astrocytes were quantified in the same brain regions, but prefrontal cortex was used instead of frontal cortex. The percentage of GFP-positive cells that colocalized with each antigen was quantified, as well as the percentage of GFP-positive cells that were astrocytes by morphology, and averages were calculated. In GFAP/Sox9 images, 22.2% of GFP-positive cells that colocalized with GFAP did not have a Sox9-positive/DAPI-positive nucleus in the plane of section and thus were not counted as astrocytes. The number of astrocytes identified by morphology in NeuN and MBP/APC images was thus corrected for astrocytes with out-of-plane cell bodies by decreasing the count by 22.2%.

Relative transduction of excitatory and inhibitory cortical neurons was quantified in 40-μm sagittal brain sections stained against GFP, VGluT1/2, GABA, and DAPI (Fig. 1G). The three rats in the inverted cohort with total GFP expression closest to the mean were used for analysis. Z-stacks of thin optical slices acquired with structured illumination were used for quantification. All GFP-positive cells with a DAPI-positive nucleus in the stack were quantified. One z-stack from frontal, parietal, temporal, and entorhinal cortex was quantified for each animal (12 stacks in total). Within each stack, the number of GFP-positive cells that colocalized with VGluT1/2, colocalized with GABA, or colocalized with neither antigen was counted. Cells with astrocytic morphology were not counted. Because oligodendrocytes and neurons could not be distinguished by morphology, the number of GFP-positive oligodendrocytes in each stack was estimated to be 4.39% of all GFP-positive cells (see above). This number was subtracted from the number of uncolocalized GFP-positive cells to obtain the number of uncolocalized GFP-positive neurons. From these counts, the average percentage of GFP-positive neurons that colocalized with VGluT1/2, GABA, or neither antigen was calculated.

Transduction of dopaminergic or cholinergic neurons was quantified in 40-μm sagittal brain sections stained against GFP, NeuN, and DAPI, as well as TH for dopaminergic neurons or the low-affinity nerve growth factor receptor (p75) for cholinergic neurons (Fig. 1, E and F). The three rats in the inverted cohort with total GFP expression closest to the mean were used for analysis. Dopaminergic transduction was quantified in SN, VTA, and the arcuate nucleus of hypothalamus. Cholinergic transduction was quantified in HDB and MS/VDB. Brain regions were identified using a rat brain atlas (*42*), and the number of cholinergic or dopaminergic neurons was counted within the entire brain region, as well as the number of GFP-positive neurons that did or did not colocalize with TH or p75. Every section containing the brain region of interest from a single series was quantified: two sections per series for SN, two for VTA, one for hypothalamus, two for HDB, and one for MS/VDB. The average percentage of cholinergic or dopaminergic neurons that were GFP-positive in each brain region was quantified for each animal, and the average among the three rats was calculated.

Statistics

It was hypothesized that gene transfer to the brain would be greater in rats from the inverted and rotated cohorts than in rats from the upright cohort. To test this hypothesis, a Friedman test was performed, comparing the mean number of GFP-positive cells in each brain region as a repeated measure across the three cohorts (n = 9 brain regions), followed by Tukey's post hoc tests. The Friedman test was used because the D'Agostino-Pearson normality test indicated that the data were nonparametric. Further, it was hypothesized that gene transfer to the following brain regions would be greater in rats from the inverted and rotated cohorts than in rats from the upright cohort: entorhinal, prefrontal, frontal, parietal, and limbic cortices, as well as hippocampus, subiculum, HDB, and MS/VDB. To test these hypotheses, a two-tailed one-way ANOVA was performed for each brain region, comparing the number of GFP-positive cells in one 40-μm section among n = 7 animals per group, followed by Tukey's post hoc tests. Data were confirmed to be normally distributed by the Shapiro-Wilk normality test.

It was also hypothesized that rats from the inverted and rotated cohorts would exhibit greater gene expression in cervical and thoracic

spinal cord than rats from the upright cohort, and that rats from the inverted cohort would exhibit greater gene expression in cervical spinal cord than in lumbar and sacral spinal cord. To test these hypotheses, a two-tailed two-way ANOVA was performed comparing the average number of GFP-positive cells within three 40-μm spinal cord sections among four different spinal levels and three groups ($n = 7$ animals per group), followed by Tukey's post hoc tests.

Last, it was hypothesized that rats from the inverted and rotated cohorts would exhibit greater gene expression in cervical DRGs than rats from the upright cohort. To test this hypothesis, a two-tailed one-way ANOVA was performed comparing the average percentage of DRG neurons that were GFP positive within three 20-μm DRG sections among $n = 7$ animals from the inverted and rotated groups and $n = 6$ animals from the upright group, followed by Tukey's post hoc tests. One animal was excluded from the upright group because sections with at least 150 neurons from three different DRGs were not obtained (see above). Data were confirmed to be normally distributed by the Shapiro-Wilk normality test.

SUPPLEMENTARY MATERIALS

Supplementary material for this article is available at http://advances.sciencemag.org/cgi/content/full/4/11/eaau9859/DC1

Fig. S1. Intrathecal AAV9 infusion does not cause microglial activation or astrogliosis.

Fig. S2. Inversion and rotation increase gene transfer to cervical spinal cord but not to other spinal levels.

Fig. S3. Transduced cells are evenly distributed after intracortical AAV9 injection.

REFERENCES AND NOTES

1. M. G. Kaplitt, P. Leone, R. J. Samulski, X. Xiao, D. W. Pfaff, K. L. O'Malley, M. J. During, Long-term gene expression and phenotypic correction using adeno-associated virus vectors in the mammalian brain. *Nat. Genet.* **8**, 148–154 (1994).
2. J. H. Kordower, C. D. Herzog, B. Dass, R. A. Bakay, J. Stansell III, M. Gasmi, R. T. Bartus, Delivery of neurturin by AAV2 (CERE-120)-mediated gene transfer provides structural and functional neuroprotection and neurorestoration in MPTP-treated monkeys. *Ann. Neurol.* **60**, 706–715 (2006).
3. W. J. Marks Jr., R. T. Bartus, J. Siffert, C. S. Davis, A. Lozano, N. Boulis, J. Vitek, M. Stacy, D. Turner, L. Verhagen, R. Bakay, R. Watts, B. Guthrie, J. Jankovic, R. Simpson, M. Tagliati, R. Alterman, M. Stern, G. Baltuch, P. A. Starr, P. S. Larson, J. L. Ostrem, J. Nutt, K. Kieburtz, J. H. Kordower, C. W. Olanow, Gene delivery of AAV2-neurturin for Parkinson's disease: A double-blind, randomised, controlled trial. *Lancet Neurol.* **9**, 1164–1172 (2010).
4. S. J. Gray, S. Nagabhushan Kalburgi, T. J. McCown, R. Jude Samulski, Global CNS gene delivery and evasion of anti-AAV-neutralizing antibodies by intrathecal AAV administration in non-human primates. *Gene Ther.* **20**, 450–459 (2013).
5. L. Samaranch, E. A. Salegio, W. San Sebastian, A. P. Kells, J. R. Bringas, J. Forsayeth, K. S. Bankiewicz, Strong cortical and spinal cord transduction after AAV7 and AAV9 delivery into the cerebrospinal fluid of nonhuman primates. *Hum. Gene Ther.* **24**, 526–532 (2013).
6. L. Samaranch, E. A. Salegio, W. San Sebastian, A. P. Kells, K. D. Foust, J. R. Bringas, C. Lamarre, J. Forsayeth, B. K. Kaspar, K. S. Bankiewicz, Adeno-associated virus serotype 9 transduction in the central nervous system of nonhuman primates. *Hum. Gene Ther.* **23**, 382–389 (2012).
7. T. Bucher, L. Dubreil, M. A. Colle, M. Maquigneau, J. Deniaud, M. Ledevin, P. Moullier, B. Joussemet, Intracisternal delivery of AAV9 results in oligodendrocyte and motor neuron transduction in the whole central nervous system of cats. *Gene Ther.* **21**, 522–528 (2014).
8. C. Hinderer, P. Bell, N. Katz, C. H. Vite, J.-P. Louboutin, E. Bote, H. Yu, Y. Zhu, M. L. Casal, J. Bagel, P. O'Donnell, P. Wang, M. E. Haskins, T. Goode, J. M. Wilson, Evaluation of intrathecal routes of administration for adeno-associated viral vectors in large animals. *Hum. Gene Ther.* **29**, 15–24 (2018).
9. J. Hordeaux, L. Dubreil, J. Deniaud, F. Iacobelli, S. Moreau, M. Ledevin, C. Le Guiner, V. Blouin, J. Le Duff, A. Mendes-Madeira, F. Rolling, Y. Cherel, P. Moullier, M. A. Colle, Efficient central nervous system AAVrh10-mediated intrathecal gene transfer in adult and neonate rats. *Gene Ther.* **22**, 316–324 (2015).
10. D. J. Schuster, J. A. Dykstra, M. S. Riedl, K. F. Kitto, L. R. Belur, R. S. McIvor, R. P. Elde, C. A. Fairbanks, L. Vulchanova, Biodistribution of adeno-associated virus serotype 9 (AAV9) vector after intrathecal and intravenous delivery in mouse. *Front. Neuroanat.* **8**, 42 (2014).
11. K. Bey, C. Ciron, L. Dubreil, J. Deniaud, M. Ledevin, J. Cristini, V. Blouin, P. Aubourg, M. A. Colle, Efficient CNS targeting in adult mice by intrathecal infusion of single-stranded AAV9-GFP for gene therapy of neurological disorders. *Gene Ther.* **24**, 325–332 (2017).
12. Y. Matsuzaki, A. Konno, R. Mukai, F. Honda, M. Hirato, Y. Yoshimoto, H. Hirai, Transduction profile of the marmoset central nervous system using adeno-associated virus serotype 9 vectors. *Mol. Neurobiol.* **54**, 1745–1758 (2017).
13. K. Meyer, L. Ferraiuolo, L. Schmelzer, L. Braun, V. McGovern, S. Likhite, O. Michels, A. Govoni, J. Fitzgerald, P. Morales, K. D. Foust, J. R. Mendell, A. H. Burghes, B. K. Kaspar, Improving single injection CSF delivery of AAV9-mediated gene therapy for SMA: A dose-response study in mice and nonhuman primates. *Mol. Ther.* **23**, 477–487 (2015).
14. S. J. Gray, V. Matagne, L. Bachaboina, S. Yadav, S. R. Ojeda, R. J. Samulski, Preclinical differences of intravascular AAV9 delivery to neurons and glia: A comparative study of adult mice and nonhuman primates. *Mol. Ther.* **19**, 1058–1069 (2011).
15. X. Xu, K. D. Roby, E. M. Callaway, Immunochemical characterization of inhibitory mouse cortical neurons: Three chemically distinct classes of inhibitory cells. *J. Comp. Neurol.* **518**, 389–404 (2010).
16. J. DeFelipe, I. Fariñas, The pyramidal neuron of the cerebral cortex: Morphological and chemical characteristics of the synaptic inputs. *Prog. Neurobiol.* **39**, 563–607 (1992).
17. M. L. Bangaru, J. Meng, D. J. Kaiser, H. Yu, G. Fischer, Q. H. Hogan, A. Hudmon, Differential expression of CaMKII isoforms and overall kinase activity in rat dorsal root ganglia after injury. *Neuroscience* **300**, 116–127 (2015).
18. L. Vulchanova, D. J. Schuster, L. R. Belur, M. S. Riedl, K. M. Podetz-Pedersen, K. F. Kitto, G. L. Wilcox, R. S. McIvor, C. A. Fairbanks, Differential adeno-associated virus mediated gene transfer to sensory neurons following intrathecal delivery by direct lumbar puncture. *Mol. Pain* **6**, 31 (2010).
19. D. J. Fink, J. Wechuck, M. Mata, J. C. Glorioso, J. Goss, D. Krisky, D. Wolfe, Gene therapy for pain: Results of a phase I clinical trial. *Ann. Neurol.* **70**, 207–212 (2011).
20. D. A. Warrell, T. M. Cox, J. D. Firth, *Oxford Textbook of Medicine* (Oxford Univ. Press, ed. 5, 2010).
21. I. Gritti, P. Henny, F. Galloni, L. Mainville, M. Mariotti, B. E. Jones, Stereological estimates of the basal forebrain cell population in the rat, including neurons containing choline acetyltransferase, glutamic acid decarboxylase or phosphate-activated glutaminase and colocalizing vesicular glutamate transporters. *Neuroscience* **143**, 1051–1064 (2006).
22. T. Sen, A. F. Esmer, H. I. Acar, S. T. Karahan, E. Tuccar, Arterial vascularisation of the anterior perforated substance. *Singapore Med. J.* **52**, 410–414 (2011).
23. G. Murlidharan, A. Crowther, R. A. Reardon, J. Song, A. Asokan, Glymphatic fluid transport controls paravascular clearance of AAV vectors from the brain. *JCI Insight* **1**, e88034 (2016).
24. K. D. Foust, E. Nurre, C. L. Montgomery, A. Hernandez, C. M. Chan, B. K. Kaspar, Intravascular AAV9 preferentially targets neonatal neurons and adult astrocytes. *Nat. Biotechnol.* **27**, 59–65 (2009).
25. J. R. Mendell, S. Al-Zaidy, R. Shell, W. D. Arnold, L. R. Rodino-Klapac, T. W. Prior, L. Lowes, L. Alfano, K. Berry, K. Church, J. T. Kissel, S. Nagendran, J. L'Italien, D. M. Sproule, C. Wells, J. A. Cardenas, M. D. Heitzer, A. Kaspar, S. Corcoran, L. Braun, S. Likhite, C. Miranda, K. Meyer, K. D. Foust, A. H. M. Burghes, B. K. Kaspar, Single-dose gene-replacement therapy for spinal muscular atrophy. *N. Engl. J. Med.* **377**, 1713–1722 (2017).
26. J. H. Kordower, M. E. Emborg, J. Bloch, S. Y. Ma, Y. Chu, L. Leventhal, J. McBride, E.-Y. Chen, S. Palfi, B. Z. Roitberg, W. D. Brown, J. E. Holden, R. Pyzalski, M. D. Taylor, P. Carvey, Z. Ling, D. Trono, P. Hantraye, N. Déglon, P. Aebischer, Neurodegeneration prevented by lentiviral vector delivery of GDNF in primate models of Parkinson's disease. *Science* **290**, 767–773 (2000).
27. A. H. Nagahara, D. A. Merrill, G. Coppola, S. Tsukada, B. E. Schroeder, G. M. Shaked, L. Wang, A. Blesch, A. Kim, J. M. Conner, E. Rockenstein, M. V. Chao, E. H. Koo, D. Geschwind, E. Masliah, A. A. Chiba, M. H. Tuszynski, Neuroprotective effects of brain-derived neurotrophic factor in rodent and primate models of Alzheimer's disease. *Nat. Med.* **15**, 331–337 (2009).
28. M. H. Tuszynski, L. Thal, M. Pay, D. P. Salmon, H. S. U, R. Bakay, P. Patel, A. Blesch, H. L. Vahlsing, G. Ho, G. Tong, S. G. Potkin, J. Fallon, L. Hansen, E. J. Mufson, J. H. Kordower, C. Gall, J. Conner, A phase 1 clinical trial of nerve growth factor gene therapy for Alzheimer disease. *Nat. Med.* **11**, 551–555 (2005).
29. K. S. Bankiewicz, J. Forsayeth, J. L. Eberling, R. Sanchez-Pernaute, P. Pivirotto, J. Bringas, P. Herscovitch, R. E. Carson, W. Eckelman, B. Reutter, J. Cunningham, Long-term clinical improvement in MPTP-lesioned primates after gene therapy with AAV-hAADC. *Mol. Ther.* **14**, 564–570 (2006).
30. K. Y. Chan, M. J. Jang, B. B. Yoo, A. Greenbaum, N. Ravi, W. L. Wu, L. Sánchez-Guardado, C. Lois, S. K. Mazmanian, B. E. Deverman, V. Gradinaru, Engineered AAVs for efficient noninvasive gene delivery to the central and peripheral nervous systems. *Nat. Neurosci.* **20**, 1172–1179 (2017).
31. B. E. Deverman, P. L. Pravdo, B. P. Simpson, S. R. Kumar, K. Y. Chan, A. Banerjee, W. L. Wu, B. Yang, N. Huber, S. P. Pasca, V. Gradinaru, Cre-dependent selection yields AAV variants for widespread gene transfer to the adult brain. *Nat. Biotechnol.* **34**, 204–209 (2016).

32. Y. Matsuzaki, A. Konno, R. Mochizuki, Y. Shinohara, K. Nitta, Y. Okada, H. Hirai, Intravenous administration of the adeno-associated virus-PHP.B capsid fails to upregulate transduction efficiency in the marmoset brain. *Neurosci. Lett.* **665**, 182–188 (2018).
33. J. Hordeaux, Q. Wang, N. Katz, E. L. Buza, P. Bell, J. M. Wilson, The neurotropic properties of AAV-PHP.B are limited to C57BL/6J mice. *Mol. Ther.* **26**, 664–668 (2018).
34. ClinicalTrials.gov, Study of Intrathecal Administration of AVXS-101 for Spinal Muscular Atrophy (STRONG), https://clinicaltrials.gov/ct2/show/NCT03381729 [accessed 25 August 18].
35. ClinicalTrials.gov, Intrathecal Administration of scAAV9/JeT-GAN for the Treatment of Giant Axonal Neuropathy, https://clinicaltrials.gov/ct2/show/NCT02362438 [accessed 25 August 2018].
36. H. Fu, J. Muenzer, R. J. Samulski, G. Breese, J. Sifford, X. Zeng, D. M. McCarty, Self-complementary adeno-associated virus serotype 2 vector: Global distribution and broad dispersion of AAV-mediated transgene expression in mouse brain. *Mol. Ther.* **8**, 911–917 (2003).
37. L. Xie, H. Kang, Q. Xu, M. J. Chen, Y. Liao, M. Thiyagarajan, J. O'Donnell, D. J. Christensen, C. Nicholson, J. J. Iliff, T. Takano, R. Deane, M. Nedergaard, Sleep drives metabolite clearance from the adult brain. *Science* **342**, 373–377 (2013).
38. A. H. Nagahara, M. Mateling, I. Kovacs, L. Wang, S. Eggert, E. Rockenstein, E. H. Koo, E. Masliah, M. H. Tuszynski, Early BDNF treatment ameliorates cell loss in the entorhinal cortex of APP transgenic mice. *J. Neurosci.* **33**, 15596–15602 (2013).
39. N. Carty, K. R. Nash, M. Brownlow, D. Cruite, D. Wilcock, M. L. Selenica, D. C. Lee, M. N. Gordon, D. Morgan, Intracranial injection of AAV expressing NEP but not IDE reduces amyloid pathology in APP+PS1 transgenic mice. *PLOS ONE* **8**, e59626 (2013).
40. L. Zhao, A. J. Gottesdiener, M. Parmar, M. Li, S. M. Kaminsky, M. J. Chiuchiolo, D. Sondhi, P. M. Sullivan, D. M. Holtzman, R. G. Crystal, S. M. Paul, Intracerebral adeno-associated virus gene delivery of apolipoprotein E2 markedly reduces brain amyloid pathology in Alzheimer's disease mouse models. *Neurobiol. Aging* **44**, 159–172 (2016).
41. Cold Spring Harbor Protocols, Mowiol embedding medium, http://cshprotocols.cshlp.org/content/2010/1/pdb.rec12110.full [accessed 25 August 2018].
42. G. Paxinos, C. Watson, *The Rat Brain in Stereotaxic Coordinates* (Academic Press, ed. 6, 2007).

Acknowledgments: We thank A. F. Adler, C. A. Lee-Kubli, J. N. Dulin, D. Gibbs, T. L. Grider, I. Kovacs, H. Kumamaru, A. H. Nagahara, and J. L. Weber for scientific and technical guidance; J. D. Ong for laboratory assistance; and A. M. Castle for graphical design assistance. **Funding:** This project was supported by the Veteran's Administration; NIH awards AG10435 (to M.H.T.), AG043416 (to M.H.T.), T32AG000216 (to M.J.C.), and R01NS099371 (to A.A.); and the Alzheimer's Association Zenith Award (to M.H.T.) and Alzheimer's Association Research Fellowship 16-443284 (to M.J.C.). **Author contributions:** M.J.C. and M.H.T. designed experiments and wrote the manuscript. M.J.C. and Y.C. conducted experiments and acquired and analyzed data. A.A. generated recombinant AAV vectors. M.H.T. supervised the project. **Competing interests:** The authors declare that they have no competing interests. **Data and materials availability:** All data needed to evaluate the conclusions in the paper are present in the paper and/or the Supplementary Materials. Additional data related to this paper may be requested from the authors.

Submitted 2 August 2018
Accepted 15 October 2018
Published 14 November 2018
10.1126/sciadv.aau9859

Citation: M. J. Castle, Y. Cheng, A. Asokan, M. H. Tuszynski, Physical positioning markedly enhances brain transduction after intrathecal AAV9 infusion. *Sci. Adv.* **4**, eaau9859 (2018).